Matrix-Isolation Infrared Spectroscopy of the Rotational Isomers of 1,2-, 1,3-, and 1,4-Benzenedicarboxaldehyde

Keiichi Ohno[†] and Takao Itoh*[,‡]

Department of Chemistry, Graduate School of Science, Hiroshima University, 1-3-1 Kagamiyama, Higashi-Hiroshima City, 739-8526, Japan, and Graduate School of Integrated Arts and Sciences, Hiroshima University, 1-7-1 Kagamiyama, Higashi-Hiroshima City, 739-8521, Japan

Received: February 16, 2007; In Final Form: April 23, 2007

Rotational isomers (rotamers) of the three structural isomers of benzenedicarboxaldehydes (1,2-, 1,3-, and 1,4-derivatives) have been investigated in detail using matrix-isolation infrared spectroscopy in the 600−4000 cm^{-1} region, combined with UV photoexcitation and density-functional theory (DFT) calculations. Two rotamers were identified for 1,2- and 1,4-benzenedicarboxaldehyde (1,2- and 1,4-BDA, respectively), while three rotamers were identified for 1,3-benzenedicarboxaldehyde (1,3-BDA) in infrared spectra upon UV-irradiation. Most of the observed infrared bands of each rotamer have been assigned. The energetic relationships among the rotamers were revealed based on the infrared data and the DFT calculations. It is shown that the intramolecular C−H···H−C interaction in the H-syn rotamer or the C−H···O═C hydrogen bonding in the anti rotamer of 1,2-BDA results in the blue-shift of the aldehyde C−H stretching band and the shortening of the aldehyde C−H bond length. Both photoinduced rotational isomerization and rearrangement were observed upon UV irradiation for 1,2-BDA. The structure of the major enol isomer formed as the result of the photochemical rearrangement of 1,2-BDA is determined.

1. Introduction

There are two possible rotamers, anti and syn, for 1,4-benzenedicarboxaldehyde (1,4-BDA) and three rotamers (anti, H-syn, and O-syn) for 1,2- and 1,3-benzenedicarboxaldehyde (1,2- and 1,3-BDA, respectively) as illustrated in Figure 1. 1,2-, 1,3-, and 1,4-BDA are also called phthalaldehyde, isophtalaldehyde, and terephthalaldehyde, respectively. The presence of the two rotamers has been indicated by NMR, infrared, Raman, and dipole moment measurements for 1,4-BDA[1−7] and by NMR for 1,2- and 1,3-BDA.[8−10] Infrared spectral data have been reported also for 1,2- and 1,3-BDA.[11−13] However, the definite spectroscopic separation and the band assignments have not been carried out for the rotamers of 1,2- and 1,3-BDA. Further, the detailed information on the energetic relationships among the rotamers was not available for 1,2- and 1,4-BDA, and infrared spectroscopy has so far not provided any evidence for the existence of the three rotamers for 1,3-BDA. The purpose of the present work is to separate and assign the infrared bands of each rotamer and to clarify the energetic relationships among the rotamers of benzenedicarboxaldehydes. In particular, it is of interest to see the spectral separability of the three rotamers for 1,2- and 1,3-BDA and to know the relative total energies among them.

In the present study, the coexistence of the three rotamers has been confirmed for 1,3-BDA and two rotamers were identified for 1,2- and 1,4-BDA through matrix-isolation infrared spectroscopy combined with UV photoexcitation as well as density functional calculations. Most of the observed bands for each rotamer have been assigned. The energetic relationships among the rotamers were revealed based on the infrared data and the DFT calculations. With 1,2-BDA, the formation of the intramolecular C−H···H−C of the H-syn rotamer or the C−H·

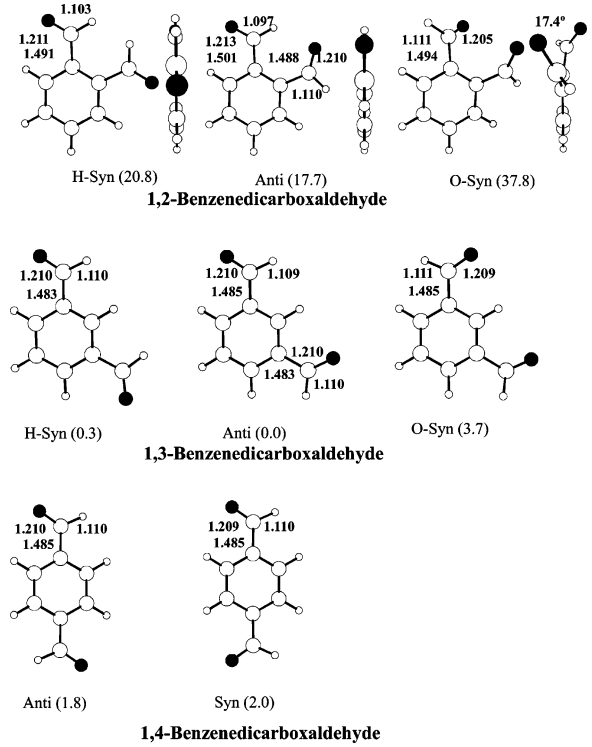

Figure 1. Geometries for 1,2-, 1,3-, and 1,4-BDA optimized at the B3LYP/6-311++G(d,p) level. The front (left) and side (right) views are shown for 1,2-BDA. Oxygen atoms are indicated by closed spheres. The relative energies (kJ mol^{-1}) of the rotamers are given in parentheses.

* To whom correspondence should be addressed. E-mail: titoh@hiroshima-u.ac.jp.
[†] Department of Chemistry, Hiroshima University.
[‡] Graduate School of Integrated Arts and Sciences, Hiroshima University.

10.1021/jp071330+ CCC: $37.00 © 2007 American Chemical Society
Published on Web 06/29/2007

···O═C hydrogen bonding of the anti rotamer results in the shortening of the aldehyde C−H bond length, which gives rise to a blue-shift of the C−H stretching band. Both the photoinduced rotational isomerization and rearrangement to an enol were observed for 1,2-BDA upon UV irradiation. The structure of the major enol photoproduct of 1,2-BDA was determined.

2. Experimental and Calculation Methods

1,2-, 1,3-, and 1,4-Benzenedicarboxaldehyde (1,2-, 1,3-, and 1,4-BDA), obtained from Aldrich, USA, were purified by means of repeated recrystallization from hexane. The gas mixture of BDA and Ar was prepared by passing pure Ar gas, obtained from Nippon Sanso, Japan (99.9999% purity), through the glass tube containing the solid BDA sample in a vacuum system at 298 K and was slowly deposited onto a CsI plate cooled to 15 K by an Iwatani Cryomini D510 refrigerator. The BDA/Ar ratio in the matrixes was approximately 1/500. The temperature of the Ar matrix was controlled by a thermostabilizer (Iwatani, TCU-4) using a PID action method and was monitored continuously by an Au-Chromel thermocouple. Infrared absorption spectra were measured with a JASCO FT/IR-615 Fourier-transform spectrophotometer equipped with a MCT detector. The infrared spectra were obtained by coaddition of 100 scans with a resolution of 1.0 cm^{-1}. In the sample conditions mentioned above, the populations of the rotamers frozen at 15 K just after the deposition are considered to be the same as those of the vapor samples at 298 K just before the deposition.[14,15] The effect of photoexcitation was examined by irradiating the deposited samples with UV light for 10 min. A superhigh-pressure mercury lamp (Ushio, SX-UI 501HQ) was used as a UV light source combined with a water filter to avoid thermal radiation and with short-wavelength cutoff filters, Sigma UTF-30U ($\lambda > 300$ nm), UTF-34U ($\lambda > 340$ nm), and UTF-37U ($\lambda > 370$ nm). UV-absorption spectra were measured with a Shimadzu UV-2550 spectrophotometer.

The quantum chemical calculations were carried out using the GAUSSIAN 03 program.[16] Optimized geometries, relative zero-point corrected energies, harmonic wavenumbers, infrared-band intensities, and natural-bond orbital (NBO) donor−acceptor perspectives of the rotamers were obtained by density-functional theory (DFT) calculations using the 6-311++G(d,p) basis set. We have used Becke's three-parameter exchange functional for the DFT calculations,[17] together with the correlation functional of Lee−Yang−Parr (B3LYP).[18] The harmonic wavenumbers ν_{harm} were scaled by the relation, $\nu_{calc} = \nu_{harm} \times (1.0087 - 0.0000163 \times \nu_{harm})$, to reproduce the anharmonicity of observed vibrations.[19,20]

3. Results and Discussion

The optimized geometries of the three rotamers of 1,2- and 1,3-BDA and the two rotamers of 1,4-BDA obtained by the DFT calculations at the B3LYP/6-311++G(d,p) level are shown in Figure 1. Each of the optimized geometries is almost planar except for the O-syn rotamer of 1,2-BDA, for which the two aldehyde groups are tilted due to the repulsion between the two oxygen atoms. The 42 fundamentals are divided into 29 of the in-plane modes and 13 of the out-of-plane modes for all the rotamers with C_s, C_{2v}, or C_{2h} symmetry except for the O-syn rotamer of 1,2-BDA. The observed and calculated wavenumbers, ν_{calc}, in the 600−1800 cm^{-1} region of 1,2-, 1,3-, and 1,4-BDA are given in Tables 1, 2, and S1, respectively, along with abbreviated assignments. The assignments were carried out in light of the measured spectra and the difference spectra between the spectra obtained before and after UV irradiation as well as the results of the DFT calculations. In particular, the comparison between the spectral patterns of the observed and calculated difference spectra was utilized as the key to the assignments.

3.1. Infrared-Band Assignments. In Figure 2, we show the observed and calculated matrix-isolation infrared spectra of 1,2-BDA. Figure 2b shows the difference spectrum, where the spectrum obtained before UV irradiation shown in Figure 2a is subtracted from that obtained after UV irradiation ($\lambda > 370$ nm). The downward and upward bands are associated, respectively, with the bands decreased and increased upon UV irradiation. The comparison of the calculated and observed spectra shows that the bands that decreased and increased upon UV irradiation belong, respectively, to the anti and H-syn rotamers of 1,2-BDA, except for several upward bands which are assigned to photoproducts.[27] Presumably, because of the large energy differences between the O-syn and the other two rotamers, we could not have obtained the evidence showing the existence of the O-syn rotamer of 1,2-BDA, and the observed bands can be safely assigned based on the two rotamers, anti and H-syn. In fact, the results of the DFT calculation show that the anti rotamer is more stable than the O-syn rotamer by 20.1 kJ mol^{-1} (1680 cm^{-1}) which corresponds to the O-syn/anti population ratio of 0.0003/1 at 298 K. This fairly large energy difference between the anti and O-syn rotamers is considered to be due to the stabilization of the intramolecular C−H···O hydrogen bond of the anti rotamer as well as the destabilization by the repulsion between the two aldehyde groups of the O-syn rotamer. The results of DFT calculation show that the anti rotamer is more stable than the H-syn rotamer by 3.1 kJ mol^{-1} (259 cm^{-1}), which corresponds to a H-syn/anti population ratio of 0.29/1 at 298 K. The barrier height from the anti to the H-syn rotamer of 1,2-BDA is calculated to be 23.0 kJ mol^{-1} (1923 cm^{-1}), indicating that the conversion between the anti and H-syn rotamers is not expected to occur at 15 K.

In Figure 3, we show the observed and calculated matrix-isolation infrared spectra of 1,3-BDA. Figure 3b shows the difference spectrum, where the spectrum obtained before UV irradiation shown in Figure 3a is subtracted from that obtained after UV irradiation ($\lambda > 300$ nm). That is, downward and upward bands are associated, respectively, with the bands that decreased and increased upon UV irradiation. With 1,3-BDA, the situation is somewhat more complicated, since three stable rotamers coexist. The comparison of the calculated difference spectra with the observed ones shows that the bands that decreased upon UV irradiation belong to the anti and H-syn rotamers, while those that increased upon UV irradiation belong to the O-syn rotamer. This is consistent with the results of the DFT calculation that the anti and H-syn rotamers are more stable than the O-syn rotamer by 3.7 kJ mol^{-1} (309 cm^{-1}) and 3.4 kJ mol^{-1} (284 cm^{-1}), respectively, which correspond to the O-syn/anti and O-syn/H-syn population ratios of 0.22/1 and 0.25/1 at 298 K. The barrier heights from the anti to H-syn rotamer and the anti to O-syn rotamer are both calculated to be 33.9 kJ mol^{-1} (2834 cm^{-1}).

Figure 4 shows the observed and calculated matrix-isolation infrared spectra of 1,4-BDA, where the downward and upward bands of the calculated spectrum are those of the anti and syn rotamers, respectively. Quite recently, Konopacka et al. reported the infrared spectrum of 1,4-BDA in an Ar matrix along with the results of DFT calculations and estimated the anti−syn energy difference and rotational barrier.[1] However, the unambiguous spectroscopic separation of each rotamer has not been reported for 1,4-BDA. The spectrum in Figure 4a is in good

TABLE 1: Observed and Calculated Wavenumbers of the Infrared Bands of 1,2-BDA in the 600−1800 cm^{-1} Region

1,2-BDA		H-syn		anti		
ν (obsd)	intens (obsd)[b]	ν (calc)[a]	intens (calcd)[a,c]	ν (calcd)[a]	intens (calcd)[a,c]	assignment[d]
1725.5	s			1734	312	C═O str (ip, C═O···HC)
1713.0	m	1725	93			C═O sym str (ip)
1710.1	s	1724	410			C═O antisym str (ip)
1701.9	s			1718	188	C═O str (ip)
1600.1	vw			1601	34	ring (ip)
1598.2	m	1599	84			ring (ip)
		1581	1			ring (ip)
1580.9	m			1579	31	ring (ip)
1498.5	vw	1489	1			ring (ip)
1494.2	w			1488	10	ring (ip)
1457.2	w	1455	9			CH def (ip)
1454.3	w			1455	5	CH def (ip)
1426.7	vw	1434	9			CCH sym bend (ip)
1409.6	vw			1416	3	CCH bend (ip)
1385.6	w			1390	4	CCH bend (ip, C═O···HC)
		1389	1			CCH antisym bend (ip)
		1327	0			ring (ip)
1306.5	m			1320	20	ring (ip)
1277.1	m	1277	32			ring (ip)
1269.4	m			1272	27	CH def (ip)
1200.0	m	1200	130			C−C sym str (ip)
1200.0	m	1195	13			CH def (ip)
1193.7	s			1194	83	ring (ip)
1193.7	s			1191	49	C−C antisym str (ip)
1159.4	vw	1171	21	1175	3	CH def (ip)
		1094	1			ring (ip)
1101.1	w			1107	6	ring (ip)
		1052	0	1055	0	CH def (ip)
				1032	2	CCH bend (op, C═O···HC)
		1017	0			CH def (op)
		1016	3	1016	1	CCH sym bend (op)
				1011	0	CH def (op)
		1006	0			CCH antisym bend (op)
		984	0	979	1	CH def (op)
		909	0	901	0	CH def (op)
859.6	m			862	34	ring (ip)
830.2	vw	835	11			C−C antisym str (ip)
813.8	sh,w	818	72			ring (ip)
804.2	m			807	51	C−C sym str (ip)
765.1	w	778	60			CH def (op)
759.3	m			772	63	CH def (op)
691.8	vw	701	9			ring (ip)
		698	0	705	0	ring (op)
657.1	w			666	17	ring (ip)
626.8	m			631	21	ring (ip)
621.5	w	628	15			ring (ip)

[a] Calculated at the B3LYP/6-311++G(d,p) level. [b] Intensities: vs, very strong; s, strong; m, medium; w, weak; vw, very weak; sh, shoulder. [c] Intensities in km mol^{-1}. [d] Abbreviated assignments are given: C═O sym or antisym str, C═O symmetric or antisymmetric stretching; ring, stretching and/or bending of the benzene ring; CH def, CH deformation of the benzene ring; CCH sym or antisym bend, CCH symmetric or antisymmetric bending of the aldehyde group; C−C sym or antisym str, C−C symmetric or antisymmetric stretching of Ph−CHO bond; ip, in-plane mode; op, out-of-plane mode.

agreement with that reported by Konopacka et al.[1] in that the infrared spectrum measured just after the deposition (Figure 4a) shows features of both the anti and syn rotamers of 1,4-BDA. Figure 4b shows the observed difference spectrum of 1,4-BDA, where the spectrum obtained before UV irradiation shown in Figure 4a is subtracted from that obtained after UV irradiation (λ > 300 nm). The downward and upward bands are associated, respectively, with the bands that decreased and increased upon UV irradiation. The comparison of the calculated and observed spectra revealed that the bands that decreased (downward bands) and increased (upward bands) upon UV irradiation belong to the anti and syn rotamers of 1,4-BDA, respectively. The assignments shown in Table S1 are also in agreement with the results of Konopacka et al. in that the intensity ratio of the infrared bands of the anti (trans) to those of the syn rotamer decreased with an increase in the dielectric constant of the solvent used. The results of the DFT calculation show that the anti rotamer is slightly more stable by 0.2 kJ mol^{-1} (17 cm^{-1}) than the syn rotamer, showing the syn/anti population ratio of 0.9/1 at 298 K. The barrier height from the anti to the syn rotamer is calculated to be 31.5 kJ mol^{-1} (2633 cm^{-1}) by the DFT calculation at the B3LYP/6-311++G(d,p) level. This is compared with the reported values of 33.6−38.6 kJ mol^{-1} obtained at the B3LYP/6-311+G(d,p) and B3LYP/6-31G(d,p) levels.[1] In any case, the conversion between the anti and syn rotamers is not expected to occur for 1,4-BDA at 15 K.

UV irradiation (λ > 370 or 300 nm) of the samples deposited at 15 K yields an increase of the population of the less stable rotamer. Hence, the coexistence of multiple rotamers has been confirmed for benzenedicarboxaldehydes by matrix-isolation infrared spectroscopy along with DFT calculations. Three rotamers were identified for 1,3-BDA in an Ar matrix just after the deposition, while two rotamers were identified for 1,2- and 1,4-BDA.

TABLE 2: Observed and Calculated Wavenumbers of the Infrared Bands of 1,3-BDA in the 600−1800 cm^{-1} region

1,3-BDA		anti		H-syn		O-syn		
ν (obsd)	intens (obsd)[b]	ν (calcd)[a]	intens (calcd)[a]	ν (calcd)[a]	intens (calcd)[a]	ν (calcd)[a]	intens (calcd)[a]	assignment[d]
1727.4	vs					1745	418	C═O sym str
		1738	135	1741	4			C═O sym str
						1738	114	C═O antisym str
1722.1	vs	1736	438	1733	625			C═O antisym str
1611.2	m			1611	58			ring (ip)
1607.9	m	1607	76					ring (ip)
1598.2	m					1602	99	ring (ip)
		1593	18	1588	8	1597	0	ring (ip)
1482.0	vw	1485	4	1488	11	1483	0	ring (ip)
1451.2	w	1449	17	1447	4	1452	1	CH def (ip)
1391.9	vw	1402	3	1400	0	1402	5	CCH antisym bend (ip)
1376.9	vw					1390	1	CCH sym bend (ip)
1370.7	w	1379	21	1377	24			CCH sym bend (ip)
		1340	3	1341	15	1337	1	ring (ip)
1285.3	vw	1295	15	1301	29			CH def (ip)
1269.4	w					1283	15	CH def (ip)
1245.3	vw			1245	53			ring (ip)
1234.7	m	1238	37			1231	34	ring (ip)
1167.7	vw	1177	0	1175	0	1179	1	CH def (ip)
1140.2	m			1148	121			C−C antisym str (ip)
1132.0	m	1139	125					C−C antisym str (ip)
1119.5	w					1126	145	C−C antisym str (ip)
1110.8	vw					1104	8	CH def (ip)
1079.5	vw	1097	11	1097	4			CH def (ip)
1008.1	vw					1028	4	CCH sym bend (op)
1006.7	vw	1026	4	1025	3			CCH sym bend (op)
		1021	0	1022	0	1018	0	CCH antisym bend (op)
		1006	1	1010	0	1006	0	ring (ip)
		1006	0	1007	1	997	0	CH def (op)
964.2	m					972	57	ring (ip)
		948	0	962	0			ring (ip)
944.0	vw					949	3	CH def (op)
938.2	w	942	40					CH def (op)
907.8	w			914	23			CH def (op)
		932	5	913	5	934	0	CH def (op)
				815	38			CH def (op)
805.6	w	808	38					CH def (op)
786.8	m					800	38	CH def (op)
793.1	m	797	19	797	34			C−C sym str
						766	6	C−C sym str
697.6	m			707	44			ring (op)
685.0	w	689	19					ring (op)
681.2	w					689	20	ring (op)
		662	11	685	18			ring (ip)
661.0	m					670	55	ring (ip)
		655	59					ring (ip)
648.5	vw					648	5	ring (ip)
646.5	w			647	13			ring (ip)

[a] Calculated at the B3LYP/6-311++G(d,p) level. [b] Intensities: vs, very strong; s, strong; m, medium; w, weak; vw, very weak; sh, shoulder. [c] Intensities in km mol^{-1}. [d] Abbreviated assignments are given: C═O sym or antisym str, C═O symmetric or antisymmetric stretching; ring, stretching and/or bending of the benzene ring; CH def, CH deformation of the benzene ring; CCH sym or antisym bend, CCH symmetric or antisymmetric bending of the aldehyde group; C−C sym or antisym str, C−C symmetric or antisymmetric stretching of Ph−CHO bond; ip, in-plane mode; op, out-of-plane mode.

3.2. Energetic Relationships among the Rotamers. The coexistence of multiple rotamers has been confirmed for benzenedicarboxaldehydes. If we assume that the conformational change occurs only between the two rotamers upon UV irradiation, then the increased amount of one of the rotamers should be the same as the decreased amount of another rotamer and vice versa. Thus, the initial population ratio of the two rotamers can be estimated from the following relation, using the infrared data obtained before and after UV irradiation,[21]

$$\frac{N_{\mathrm{syn}'}}{N_{\mathrm{anti}'}} = \left(\frac{\alpha_{\mathrm{anti}}}{\alpha_{\mathrm{syn}}}\right)\left(\frac{A_{\mathrm{syn}'}}{A_{\mathrm{anti}'}}\right) = -\frac{(A_{\mathrm{anti}''} - A_{\mathrm{anti}'})}{(A_{\mathrm{syn}''} - A_{\mathrm{syn}'})}\left(\frac{A_{\mathrm{syn}'}}{A_{\mathrm{anti}'}}\right) \quad (1)$$

where α_x, N_x, and A_x with x = syn or anti denote, respectively, the absorption coefficient, population, and absorbance of one of the rotamers (e.g., syn or anti), with prime and double prime denoting the samples before and after UV irradiation, respectively.

With 1,4-BDA, most of the observed bands of the two rotamers are located close to one another, in addition to the small intensity change before and after UV irradiation. Therefore, there are some difficulties for determining the accurate band-intensity ratios. We have chosen the bands at 771 (anti) and 805 (syn) cm^{-1} for the determination of the population ratio of the rotamers of 1,4-BDA, where the integrated band areas were obtained by a curve-fitting technique using Gaussian−Lorentzian functions. We obtained the $N_{\mathrm{syn}'}/N_{\mathrm{anti}'}$ value of

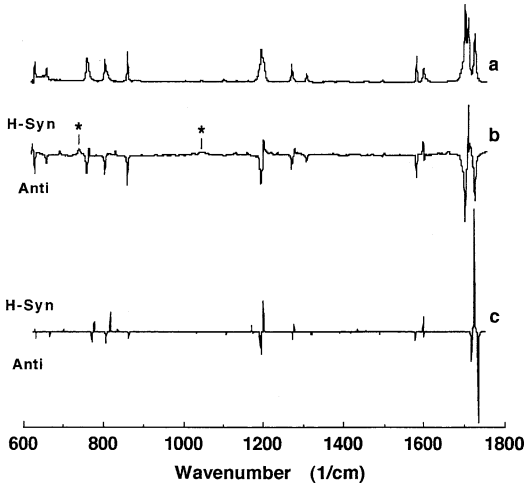

Figure 2. Observed and calculated infrared spectra of 1,2-BDA: (a) spectrum obtained immediately after the deposition of the sample at 15 K; (b) the difference spectrum, where the spectrum obtained before UV irradiation is subtracted from that obtained after UV irradiation (λ > 370 nm); (c) calculated difference spectrum, where the bands of the anti and H-syn rotamers are shown by the downward and upward bands, respectively. The bands corresponding to phthalide as one of the photoproducts are indicated by asterisks.[27]

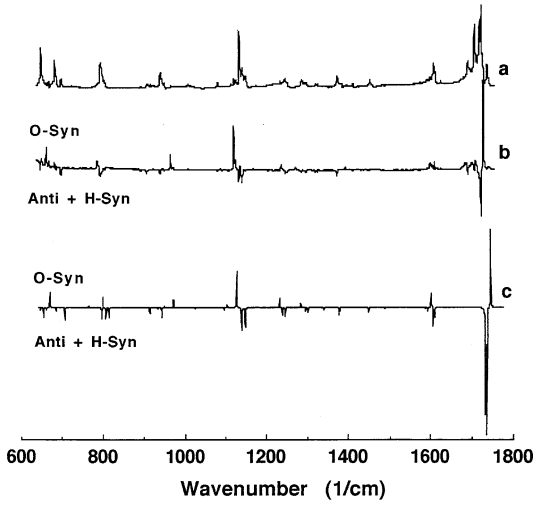

Figure 3. Observed and calculated infrared spectra of 1,3-BDA: (a) spectrum observed immediately after the deposition of the sample at 15 K; (b) the difference spectrum, where the spectrum obtained before UV irradiation is subtracted from that obtained after UV irradiation (λ > 300 nm); (c) calculated difference spectrum, where the bands of the anti and H-syn rotamers are shown by the downward bands and those of the O-syn rotamer are shown by the upward bands.

0.8 ± 0.1 for 1,4-BDA ($N_{syn'}/N_{anti'} = 1.0 \pm 0.1(A_{805}/A_{771}) = 0.8 \pm 0.1$). This value corresponds to the energy (Gibbs energy) difference, ΔG, of 0.6 ± 0.4 kJ mol^{-1} (50 ± 30 cm^{-1}) due to the relation, $\ln(N_{syn'}/N_{anti'}) = -\Delta G/RT$, with T and R denoting the absolute temperature (298 K) just before the sample deposition and the gas constant, respectively. The evaluated ΔG value is somewhat large but in the same order of magnitude as compared with 0.2 kJ mol^{-1} (17 cm^{-1}) obtained from DFT calculations at 298 K.

With 1,3-BDA, the situation is somewhat complicated, as compared with that of 1,4-BDA, because the three rotamers have been identified. Assuming that the absorption-coefficient ratio between the absorption bands of the two rotamers of 1,3-BDA are the same as those obtained from the DFT calculations, we

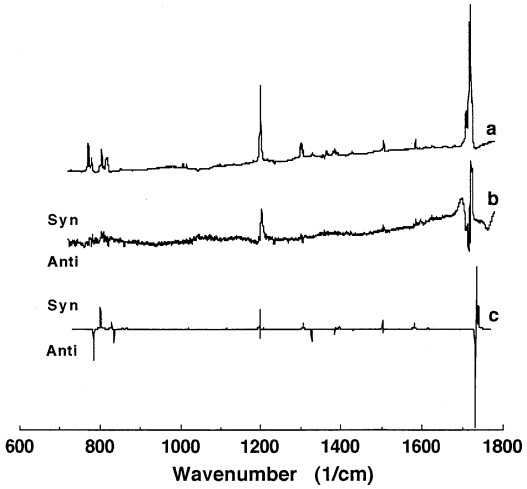

Figure 4. Observed and calculated infrared spectra of 1,4-BDA: (a) spectrum obtained immediately after the deposition of the sample at 15 K; (b) the difference spectrum, where the spectrum obtained before UV irradiation is subtracted from that obtained after UV irradiation (λ > 300 nm); (c) calculated difference spectrum, where the bands of the anti and syn rotamers are shown by the downward and upward bands, respectively.

obtain the values of 0.9 and 0.1, respectively, for the H-syn/anti and O-syn/anti population ratios, i.e.,

$$\frac{N_{\text{H-syn}'}}{N_{\text{anti}'}} = \left(\frac{\alpha_{\text{anti}}}{\alpha_{\text{H-syn}}}\right)\left(\frac{A_{\text{H-syn}'}}{A_{\text{anti}'}}\right) = 1.0\left(\frac{A_{1140}}{A_{1132}}\right) = 0.9$$

and

$$\frac{N_{\text{O-syn}'}}{N_{\text{anti}'}} = \left(\frac{\alpha_{\text{anti}}}{\alpha_{\text{O-syn}}}\right)\left(\frac{A_{\text{O-syn}'}}{A_{\text{anti}'}}\right) = 0.86\left(\frac{A_{1120}}{A_{1132}}\right) = 0.1$$

These ratios correspond to the anti − H-syn and the anti − O-syn energy differences of about 0.3 kJ mol^{-1} (20 cm^{-1}) and 5.7 kJ mol^{-1} (480 cm^{-1}), respectively, indicating that the ground-state energies of the anti and H-syn rotamers are nearly the same. Since the anti and H-syn rotamers are shown to have almost the same ground-state energies, we can estimate the O-syn/anti population ratio without the assumption of the equality between the empirical and calculated absorption coefficients. Applying a modification of eq 1, we have obtained the O-syn/anti (or O-syn/H-syn) population ratio.

$$\frac{N_{\text{O-syn}'}}{N_{\text{anti}'}} = -\frac{(A_{\text{anti}''} - A_{\text{anti}'})}{{}^1/_2(A_{\text{O-syn}''} - A_{\text{O-syn}'})}\left(\frac{A_{\text{O-syn}'}}{A_{\text{anti}'}}\right) = 0.74\left(\frac{A_{1120}}{A_{1132}}\right) = 0.10 \pm 0.01$$

or

$$\frac{N_{\text{O-syn}'}}{N_{\text{H-syn}'}} = -\frac{(A_{\text{H-syn}''} - A_{\text{H-syn}'})}{{}^1/_2(A_{\text{O-syn}''} - A_{\text{O-syn}'})}\left(\frac{A_{\text{O-syn}'}}{A_{\text{H-syn}'}}\right) = 0.99\left(\frac{A_{1120}}{A_{1140}}\right) = 0.13 \pm 0.01$$

Thus, we obtain the O-syn/anti (or O-syn/H-syn) population ratio ($N_{\text{O-syn}'}/N_{\text{anti}'}$) of 0.11 ± 0.02 which corresponds to the anti − O-syn energy difference of 5.4 ± 0.4 kJ mol^{-1} (450 ± 30 cm^{-1}). The anti − O-syn energy differences obtained by two different methods for 1,3-BDA are almost the same but are somewhat larger than the calculated value of 3.2−3.5 kJ mol^{-1} (270−290 cm^{-1}) at 298 K. However, considering the errors introduced

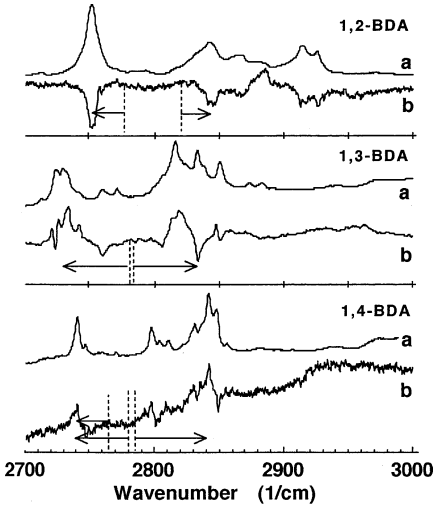

Figure 5. Observed infrared spectra of 1,2, 1,3-, and 1,4-BDA in the 2700−3000 cm^{-1} region: (a) spectra observed immediately after the deposition of the sample at 15 K; (b) difference spectra, where the spectrum obtained before UV irradiation is subtracted from that obtained after UV irradiation (λ > 300 or 370 nm). The dashed lines indicate the expected band locations without Fermi resonance.

to the evaluation of the band intensities, we can say that the empirical values are in reasonable agreement with the calculated ones.

With 1,2-BDA, eq 1 is not applicable to estimate the population ratio, since photolysis takes place in addition to isomerization. However, the population ratio can be estimated from the band intensity ratios for the sample before UV irradiation, if we assume the equality between the empirical and calculated absorption coefficients. We have chosen the bands at 860 (anti) and 830 cm^{-1} (H-syn) for the determination of the population ratio. Using the calculated absorption-coefficients ratio, $\alpha_{anti}/\alpha_{H\text{-}syn} = 3.0$, and the observed intensity ratio ($A_{H\text{-}syn}/A_{anti} = A_{830}/A_{860}$) of 0.018, we have tentatively obtained the H-syn/anti population ratio of 0.06, which corresponds to an energy difference of 6.9 kJ mol^{-1} (580 cm^{-1}). This value is also in reasonable agreement with the calculated energy difference of 5.2 kJ mol^{-1} (435 cm^{-1}) at 298 K.

3.3. Intramolecular Interactions of the anti and H-syn Rotamers of 1,2-BDA. The matrix-isolation infrared spectra of 1,2-, 1,3-, and 1,4-BDA in the 2700−3000 cm^{-1} region are shown in Figure 5, where the spectrum in part b is obtained by subtracting the spectrum before UV irradiation (part a) from that after UV irradiation. The downward and upward bands correspond, respectively, to the bands that decreased and increased upon UV irradiation. On the basis of the analyses in the 600−1800 cm^{-1} region already described, the downward bands in the spectrum of part b are definitely assigned to those of the anti rotamers for 1,2-, 1,3-, and 1,4-BDA. Several strong bands are observed separately in the 2800−2850 and 2720−2760 cm^{-1} regions for 1,3- and 1,4-BDA, although the DFT calculations show only the two aldehyde C−H stretching bands for each rotamer in the 2780−2800 cm^{-1} region. It is well-known that the aldehyde C−H stretching mode and the first overtone of the aldehyde C−H in-plane bending mode at about 1400 cm^{-1} are both in Fermi resonance.[21−24] In Table 3 we present the assignments of these vibrations based on the results of the DFT calculations along with the infrared-band intensities by considering Fermi resonance. Several unassigned bands are also seen in Figure 5. These bands are probably associated with the first overtone or combination bands for the aldehyde C−H in-plane bending bands and/or the ring vibration bands in the 1350−1480 cm^{-1} region. With 1,2-BDA, on the other hand, the bands are observed at 2914 and 2864 cm^{-1}, respectively, for the anti and H-syn rotamers in the region above 2850 cm^{-1}. These bands are assigned to the intramolecularly interacting C−H stretching band without Fermi resonance on the basis of the calculated wavenumbers of 2925 cm^{-1} for the anti rotamer and 2864 cm^{-1} for the H-syn rotamer. The blue-shifts of these bands indicate the presence of the shortened C−H bond, as will be mentioned below in more detail.

With 1,2-BDA, the two aldehyde groups are located close to each other, which is considered to induce the repulsion between the two aldehyde groups to a certain extent. In fact, the DFT calculations at the B3LYP/6-311++G(d,p) level indicate that the total energies of all the rotamers of 1,2-BDA are higher by 13−18 kJ mol^{-1} than those of 1,3- and 1,4-BDA (see Figure 1). These high total energies are most probably brought

TABLE 3: Observed and Calculated Wavenumbers of the Infrared Bands of 1,2-, 1,3-, and 1,4-BDA in the 2700−3000 cm^{-1} Region

	ν (obsd)	intens (obsd)[b]	ν (calcd)[a]	intens (calcd)[a,c]	assignment[d]
1,2-BDA	2926	w			
	2914	m	2925	17	CH str (anti, CH···O)
	2886	b, vw	2864	133	CH sym str (H-syn, CH···HC)
			2831	17	CH antisym str (H-syn, CH···HC)
	2865	b, w			
	2843	m			2 × 1410 (anti), Fermi
	2752	s	2781	106	CH str (anti), Fermi
1,3-BDA	2851	s	2794	89	CH sym str (anti), Fermi
			2784	114	CH antisym str (anti), Fermi
	2834	s	2783	200	CH sym str (H-syn), Fermi
			2781	4	CH antisym str (H-sym), Fermi
	2816	s	2781	40	CH sym str (O-syn), Fermi
			2779	192	CH antisym str (O-syn), Fermi
	2731	s			2 × 1392, 2 × 1377 (O-syn), Fermi
	2725	s			2 × 1392, 2 × 1371, 1392 + 1371 (anti, H-syn), Fermi
1,4-BDA	2848	m	2789	30	CH sym str (anti), Fermi
	2842	s	2785	137	CH sym str (syn), Fermi
	2831	m	2784	93	CH antisym str (syn), Fermi
	2798	m	2788	200	CH antisym str (anti)
	2747	w			2 × 1391, 2 × 1380 (anti), Fermi
	2741	s			2 × 1391, 2 × 1384, 1391 + 1384 (syn), Fermi

[a] Calculated at the B3LYP/6-311++G(d,p) level. [b] Intensities: b, broad; s, strong; m, medium; w, weak; vw, very weak. [c] Intensities in km mol^{-1}. [d] Abbreviated assignments are given: C−H sym or antisym str; aldehyde C−H symmetric or antisymmetric stretching; Fermi, bands in Fermi resonance.

about by the repulsion between the two adjacent aldehyde groups of 1,2-BDA. In particular for the O-syn rotamer, the two aldehyde groups are tilted against the molecular plane, showing the C═O···O═C distance of 2.945 Å (1 Å = 10^{-10} m) as shown in Figure 1. Further, the C−C bond lengths of the aldehyde groups for 1,2-BDA are also lengthened by 0.016−0.003 Å as compared with those of the rotamers of 1,3- and 1,4-BDA, presumably due to the repulsion between the two aldehyde groups. On the other hand, the C−H···H−C distance (1.986 Å) between the two aldehyde groups for the H-syn rotamer and the C−H···O═C distance (2.232 Å) between the two aldehyde groups for the anti rotamer of 1,2-BDA are shorter than the sums of the van der Waals radii of two H atoms (2.4 (= 1.2 + 1.2) Å) and of one H and one O atom (2.6 (=1.2 + 1.4) Å), respectively. These observations indicate the presence of intramolecular interactions for the anti and H-syn rotamers of 1,2-BDA.

Aiming at obtaining further information on the intramolecular interactions, we have carried out the natural bond orbital (NBO) analyses at the level equivalent to that of the DFT calculation.[16] The NBO analyses indicate that there is an intragroup interaction, $n(O) \rightarrow \sigma^*(C-H)$, in each of the two aldehyde groups of 1,3- and 1,4-BDA with a stabilization energy of about 99 kJ mol^{-1}. That is, the oxygen atom donates a part of the lone-pair electrons (n(O)) to the C−H σ antibonding orbital (σ^*(C−H)) in each of the aldehyde groups, which weakens the C−H bond strength. As a result, the C−H bond is lengthened and the C−H stretching band is red-shifted to the 2700−2850 cm^{-1} region located at energies lower than those of the C−H stretching bands observed in general for alkenes (3000−3100 cm^{-1}) and alkanes (2850−3000 cm^{-1}).

The NBO analysis of the anti rotamer of 1,2-BDA indicates the presence of an intergroup interaction between the two different aldehyde groups, $n(O^b) \rightarrow \sigma^*(C^a-H)$, with a stabilization energy of 8.8 kJ mol^{-1}. That is, one of the aldehyde groups ($-C^bHO^b$) donates a part of the lone-pair electrons ($n(O^b)$) on the oxygen atom O^b to the C^a−H σ antibonding orbital (σ^*-(C^a−H)) of another aldehyde group ($-C^aHO^a$). Thus, the analysis indicates the presence of the normal C−H···O═C hydrogen bonding with the C−H bond being lengthened due to hydrogen bonding, but at the same time the intragroup interaction, $n(O^a) \rightarrow \sigma^*(C^a-H)$, in the aldehyde group ($-C^aHO^a$) is weakened by 13 kJ mol^{-1}. Therefore, the influence of the latter interaction, $n(O_a) \rightarrow \sigma^*(C^a-H)$, exceeds that of the former interaction, $n(O^b) \rightarrow \sigma^*(C^a-H)$. As a result, the C^a−H bond is shortened.

With the H-syn rotamer of 1,2-BDA, the intergroup interactions between the two different aldehyde groups, $\sigma(C^a-H) \rightarrow \sigma^*(C^b-H)$ and $\sigma(C^b-H) \rightarrow \sigma^*(C^a-H)$, occur with each one having a stabilization energy of 2.4 kJ mol^{-1}, but at the same time the intragroup interaction in each of the aldehyde groups, $n(O) \rightarrow \sigma^*(C-H)$, is weakened by 6 kJ mol^{-1}. Thus, the influence of the interactions $n(O) \rightarrow \sigma^*(C-H)$ in each of the aldehyde groups exceeds that of the interactions between the two different aldehyde groups, $\sigma(C^a-H) \rightarrow \sigma^*(C^b-H)$ and $\sigma(C^b-H) \rightarrow \sigma^*(C^a-H)$. As the result, the two C−H bond lengths are shortened.

The C−H bond lengths of the two interacting aldehyde groups of the H-syn and anti rotamers of 1,2-BDA are calculated to be shorter by 0.007−0.013 Å than those of the benzenedicarboxaldehydes other than 1,2-BDA (1.110 Å). In accordance with Badger's rule, the stretching wavenumber is reciprocally proportional to the bond length.[25,26] Thus, the shortenings of the C−H bond lengths are caused indirectly by the formation of the intramolecular C−H···H−C interaction for the H-syn rotamer or the intramolecular C−H···O═C hydrogen bond for the anti rotamer of 1,2-BDA, resulting in the observed blue-shifts of the C−H stretching bands.

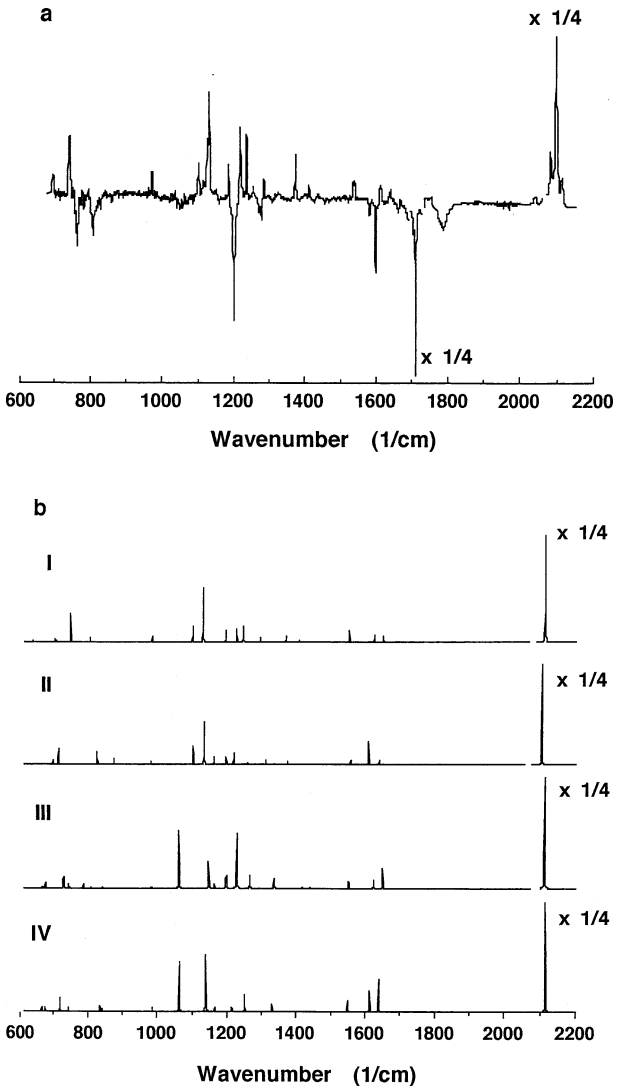

Figure 6. (a) Difference spectrum of 1,2-BDA, where the spectrum obtained after the second UV irradiation with $\lambda > 370$ nm for 10 min is subtracted from that obtained after the first UV irradiation with $\lambda >$ 300 nm. (b) Calculated infrared spectra of the possible four photoproducts (I, II, III, and IV) of 1,2-BDA.

3.4. Photolysis of 1,2-BDA and the Structures of the Photoproducts. Figure 6 shows the difference spectrum of 1,2-BDA in the 600−2200 cm^{-1} region, where the spectrum observed after the second UV irradiation with $\lambda \geq 370$ nm (323 kJ mol^{-1}) is subtracted from that after the first UV irradiation with $\lambda \geq 300$ nm (399 kJ mol^{-1}), along with the calculated spectra. The upward bands in the observed difference spectrum are the ones whose intensities increased upon the first UV irradiation. The assignments of the infrared bands of the photoproducts were carried out by referring to the DFT outputs. The characteristic strong bands observed at 3667 (and/or 3660) and 2097 cm^{-1} are assigned to the O−H stretching and the C═C═O asymmetric stretching modes, respectively. Gebicki et al. have reported an enol-type compound as the major photoproduct of 1,2-BDA.[11] Referring to their results, we have calculated the infrared spectra of the four possible enol isomers of the photoproducts (I, II, III, and IV) shown in Figure 7. The calculated spectra of I and II resemble each other, but closer

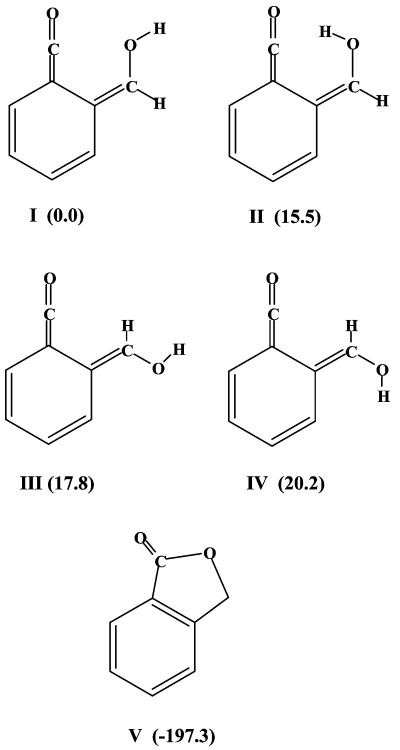

Figure 7. Chemical structures for the photoproducts of 1,2-BDA (I, II, III, IV, and V), with the relative energies (kJ/mol) obtained at the B3LYP/6-311++G(d,p) level given in parentheses.

inspection of the spectra reveals that the observed difference spectrum matches well with the calculated spectrum of the enol I with a *Z*-conformation. This result disagrees with that reported recently for the photoproducts of 1,2-BDA, for which the *E*-conformation enol (III or IV) is the major photoproduct.[27] The assignments and locations of the observed infrared bands of photoproduct I are summarized in Table S2.

We have also calculated the energies of the isomers and the transition states for the photoproducts of 1,2-BDA. The DFT calculations show that the zero-point corrected energies of I, II, III, and IV with respect to the anti rotamer of 1,2-BDA are 127.6, 143.0, 145.5, and 147.9 kJ mol^{-1}, respectively, and that the barrier heights for the transitions from the anti rotamer of 1,2-BDA to II, from I to II, from I to III, and from III to IV are 189.7, 14.4, 123.5, and 8.4 kJ mol^{-1}, respectively. These results suggest, along with the molecular structures of the photoproducts, that enol I is formed via unstable enol II from the anti rotamer. Besides enol I, we have also detected the infrared bands corresponding to a cyclic compound V (phthalide) upon irradiation with $\lambda < 370$ nm and benzaldehyde and carbon monoxide upon irradiation with $\lambda < 300$ nm as the minor photoproducts, as has been reported.[27]

The increase of the band intensities of the less stable rotamer of 1,2-BDA is observed not only upon irradiation with $\lambda > 370$ nm but upon UV irradiation with $300 < \lambda < 370$ nm. Thus, the rotational isomerization of 1,2-BDA, as well as that of 1,3- and 1,4-BDA, is considered to occur upon irradiation of the light with this wavelength region. The UV−vis absorption bands in hexane are observed at wavelengths 270−310 nm (S_2 (π, π^*)) and 320−400 nm (S_1 (n, π^*)) for 1,2-BDA, at 260−300 nm (S_2) and 300−380 nm (S_1) for 1,3-BDA, and at 270−310 nm (S_2) and 320−390 nm (S_1) for 1,4-BDA. It is inferred from these observations that a conformational change takes place presumably through the electronically excited S_1 (n, π^*) and/or S_2 (π, π^*) states. In particular for 1,2-BDA, both the photoinduced rearrangement to enol I and the rotational isomerization are observed upon UV irradiation.

4. Conclusions

Two rotamers were identified for 1,2- and 1,4-BDA, while three rotamers were identified for 1,3-BDA in the matrix-isolation infrared spectra in the 600−4000 cm^{-1} region combined with UV photoexcitation and density-functional theory calculations. Most of the observed infrared bands of each rotamer have been assigned. The energetic relationships among the rotamers were revealed based on the infrared data and the DFT calculations. On the basis of the infrared data, the energy differences are estimated to be 580, 450 ± 30, and 50 ± 30 cm^{-1}, respectively, for the anti − H-syn rotamer of 1,2-BDA, for the anti − O-syn rotamer of 1,3-BDA, and for the anti − H-syn rotamer of 1,4-BDA, with the anti rotamers being the most stable isomers. The interaction between the two aldehyde groups of 1,2-BDA is shown to result in the shortening of the aldehyde C−H bond length due to the interactions between the two closely located aldehyde groups. The photoinduced rearrangement was observed for 1,2-BDA in addition to the photoinduced rotational isomerization upon UV irradiation. The structure of the major enol photoproduct from 1,2-BDA was determined.

Acknowledgment. This work was supported in part by a Grant-in-Aid for Scientific Research (A) Grant No. 16205003 from the Ministry of Education, Culture, Sports, Science and Technology of the Japanese Government. This work was supported in part also by a grant from the Hiruma Foundation (Phos Co.) through the president of Hiroshima University.

Supporting Information Available: Tables S1 and S2 containing vibrational band assignments for 1,4-BDA and the main enol photoproduct of 1,2-BDA. This material is available free of charge via the Internet at http://pubs.acs.org.

References and Notes

(1) Konopacka, A.; Pajak, J.; Jezierska, A.; Panek, J.; Ramaekers, R.; Maes, G.; Pawelka, Z. *Struct. Chem.* **2006**, *17*, 177.
(2) Rogojerov, M.; Jordanov, B.; Keresztury, G. *J. Mol. Struct.* **2000**, *550−551*, 455.
(3) Rogojerov, M.; Jordanov, B.; Keresztury, G. *J. Mol. Struct.* **1999**, *480−481*, 153.
(4) Lamcharfi, E.; Kerbal, A.; Kunesch, G.; Meyer, C. *J. Carbohydr. Chem.* **1998**, *17*, 1015.
(5) Drakenberg, T.; Sommer, J.; Jost, R. *J. Chem. Soc., Perkin Trans. 2* **1980**, 363.
(6) Bernassau, J. M.; Drakenberg, T.; Liljefors, T. *Acta Chem. Scand.* **1977**, *B31*, 836.
(7) Lunazzi, L.; Ticca, A.; Macciantelli, D.; Spunta, G. *J. Chem. Soc., Perkin Trans. 2* **1976**, 1121.
(8) Casarini, D.; Lunazzi, L.; Mazzanti, A. *J. Org. Chem.* **1997**, *62*, 7592.
(9) Schaefer, T.; Penner, G. H.; Sebastian, R.; Takeuchi, C. S. *Can. J. Chem.* **1986**, *64*, 158.
(10) Bernassau, J. M.; Drakenberg, T.; Liljefors, T. *Acta Chem. Scand.* **1977**, *B31*, 836.
(11) Gebicki, J.; Kuberski, S. *J. Chem. Soc., Chem. Commun.* **1988**, 1364.
(12) Lal, B. B.; Srivastava, M. P.; Singh, I. S. *Indian J. Pure Appl. Phys.* **1971**, *9*, 857.
(13) Srivastava, M. P.; Lal, B. B.; Singh, I. S. *Indian J. Pure Appl. Phys.* **1972**, *10*, 570.
(14) Felder, P.; Guenthard, H. Hs. *Spectrochim. Acta, Part A* **1980**, *36*, 223.
(15) Kudoh, S.; Takayanagi, M.; Nakata, M. *Chem. Phys. Lett.* **1998**, *296*, 329.
(16) Frisch, M. J.; Trucks, G. W.; Schlegel, H. B.; Scuseria, G. E.; Robb, M. A.; Cheeseman, J. R.; Montgomery, J. A.; Vreven, T., Jr.; Kudin, K. N.; Burant, J. C.; Millam, J. M.; Iyengar, S. S.; Tomasi, J.; Barone, V.; Mennucci, B.; Cossi, M.; Scalmani, G.; Rega, N.; Petersson, G. A.;

Nakatsuji, H.; Hada, M.; Ehara, M.; Toyota, K.; Fukuda, R.; Hasegawa, J.; Ishida, M.; Nakajima, T.; Honda, Y.; Kitao, O.; Nakai, H.; Klene, M.; Li, X.; Knox, J. E.; Hratchian, H. P.; Cross, J. B.; Adamo, C.; Jaramillo, J.; Gomperts, R.; Stratmann, R. E.; Yazyev, O.; Austin, A. J.; Cammi, R.; Pomelli, C.; Ochterski, J. W.; Ayala, P. Y.; Morokuma, K.; Voth, G. A.; Salvador, P.; Dannenberg, J. J.; Zakrzewski, V. G.; Dapprich, S.; Daniels, A. D.; Strain, M. C.; Farkas, O.; Malick, D. K.; Rabuck, A. D.; Raghavachari, K.; Foresman, J. B.; Ortiz, J. V.; Cui, Q.; Baboul, A. G.; Clifford, S.; Cioslowski, J.; Stefanov B. B.; Liu, G.; Liashenko, A.; Piskorz, P.; Komaromi, I.; Martin, R. L.; Fox, D. J.; Keith, T.; Al-Laham, M. A.; Peng, C. Y.; Nanayakkara, A.; Challacombe, M.; Gill, P. M. W.; Johnson, B.; Chen, W.; Wong, M. W.; Gonzalez, C.; Pople, J. A. *Gaussian* 03, revision B.05, Gaussian, Inc.: Pittsburgh, PA, 2003.

(17) Becke, A. D. *J. Chem. Phys.* **1993**, *98*, 5648.

(18) Lee, C.; Yang, W.; Parr, R. G. *Phys. Rev. B* **1988**, *37*, 785.

(19) Yoshida, H.; Takeda, K.; Okamura, J.; Ehara, A.; Matsuura, H. *J. Phys. Chem. A* **2002**, *106*, 3580.

(20) Kudoh, S.; Takayanagi, M.; Nakata, M. *Chem. Phys. Lett*. **2000**, *328*, 363.

(21) Itoh, T.; Akai, N.; Ohno, K. *J. Mol. Struct.* **2006**, *786*, 39.

(22) Pinchas, S. *Anal. Chem*. **1957**, *29*, 334.

(23) Pinchas, S. *Anal. Chem*. **1955**, *27*, 2.

(24) Nyquist, R. A.; Settineri, S. E.; Luoma, D. A. *Appl. Spectrosc*. **1992**, *46*, 293.

(25) Badger, R. M. *J. Chem. Phys*. **1934**, *2*, 128.

(26) Kurita, E.; Matsuura, H.; Ohno, K. *Spectrochim. Acta, Part A* **2004**, *60*, 3013.

(27) Scaiano, J. C.; Encinas, V. M.; George, M. V. *J. Chem. Soc., Perkin Trans. 2* **1980**, 724.